Journal of Dental Sciences 16 (2021) 1170–1181

Available online at www.sciencedirect.com

ScienceDirect

journal homepage: www.e-jds.com

Original Article

Real-time assessment of guided bone regeneration in critical size mandibular bone defects in rats using collagen membranes with adjunct fibroblast growth factor-2

Mitsuaki Furuhata [a], Tadahiro Takayama [b,c*], Takanobu Yamamoto [b], Yasumasa Ozawa [b], Motoki Senoo [a], Manami Ozaki [d,e], Seiichi Yamano [f], Shuichi Sato [b,c]

[a] *Division of Applied Oral Sciences, Nihon University Graduate School of Dentistry, Tokyo, Japan*
[b] *Department of Periodontology, Nihon University School of Dentistry, Tokyo, Japan*
[c] *Division of Advanced Dental Treatment, Dental Research Center, Nihon University School of Dentistry, Tokyo, Japan*
[d] *Department of Oral Health Sciences, Nihon University School of Dentistry, Tokyo, Japan*
[e] *Division of Functional Morphology, Dental Research Center, Nihon University School of Dentistry, Tokyo, Japan*
[f] *Department of Prosthodontics, New York University College of Dentistry, NY, USA*

Received 2 February 2021; Final revision received 14 March 2021
Available online 3 April 2021

KEYWORDS
Bone regeneration;
Collagen membrane;
Growth factors;
Fibroblast growth factor-2;
Rat mandibular bone defects;
Real-time in vivo micro-computerized

Abstract *Background/purpose:* Fibroblast growth factor-2 (FGF-2) regulates bone formation. The concept of guided bone regeneration using a resorbable collagen membrane (RCM) is generally accepted in implant dentistry. This study aimed to investigate the bone healing pattern in rat mandibular bone defects in real-time with and without RCM containing FGF-2 (RCM/FGF-2).

Materials and methods: Critical-size circular bone defects (4.0 mm diameter) were created on both sides of the rat mandibular bone. The defects were randomly divided into the following groups: control, RCM alone, RCM containing low (0.5 μg) or high (2.0 μg) concentration of FGF-2. We performed real-time in vivo micro-computerized tomography scans at the baseline and at 2, 4, and 6 weeks, and measured the volume of newly formed bone (NFB), bone mineral density (BMD) of NFB, and the closure percentage of the NFB area. At 6 weeks, the mandibular

* Corresponding author. Department of Periodontology, Nihon University School of Dentistry, 1-8-13 Kanda-Surugadai, Chiyoda-ku, Tokyo 101-8310, Japan. Fax: +81-3-3219-8349.
E-mail address: takayama.tadahiro@nihon-u.ac.jp (T. Takayama).

https://doi.org/10.1016/j.jds.2021.03.008

tomography

specimens were assessed histologically and histomorphometrically to evaluate the area of new bone regeneration.
Results: Real-time assessment revealed a significant increase in the volume, BMD, and closure percentage of the NFB area in the RCM/FGF-2-treated groups than that in the control and RCM groups. In the H-FGF-2 group, the volume and BMD of NFB exhibited a significant increase at 6 weeks than that at the baseline. Histological evaluation revealed the presence of osteoblasts, osteocytes, and blood vessels within the NFB.
Conclusion: The real-time in vivo experiment demonstrated that RCM/FGF-2 effectively promoted bone regeneration within the critical-size mandibular defects in rats and verified new bone formation starting in the early postoperative phase.

Introduction

Rehabilitation of edentulous areas with osseointegrated implants has advanced dentistry and improved patients' quality of life.[1] However, bone loss or insufficiency remains a major challenge for bone-anchored implants. Guided bone regeneration (GBR) is the most common treatment modality for reconstructing the alveolar bone.[2]

The membrane used for GBR is an essential component of the treatment. A membrane to be used for GBR therapy should possess desirable characteristics, such as biocompatibility, cell-occlusion properties, integration with host tissues, clinical manageability, space-making capacity, and adequate mechanical and physical properties.[3] In particular, naturally derived resorbable collagen membranes (RCMs) have attracted considerable attention, because collagen is a principal component of connective tissue and provides structural support. As a biomaterial, collagen has several properties, including resorbability and low immunogenicity.[4] In bone regeneration therapy, several carrier biomaterials for GBR have been reported.[5,6] In particular, collagen-based carriers have been used more often in clinical and translational research.[7—9] Collagen promotes hemostasis by stimulating platelet attachment and increasing fibrin linkages, supports osteogenesis by providing a surface for attachment of osteoblasts, acts as a scaffold for neovascularization and increases chemotaxis for fibroblasts.[4,10] However, this material requires certain modifications for effective clinical outcomes, such as faster healing and improved quantity and quality of the resulting regenerated bone. Therefore, it is desirable to develop a membrane that also exhibits osteoinductive activity in the defects. Additional factors may contribute to bone regeneration in the defects, such as GBR with membranes and adjunct growth factors that regulate cellular events associated with tissue regeneration and repair. Application of growth factor-incorporated RCMs around the bone defects leads to complete healing of osseous defects at the GBR sites.

Recently, a study reported the ability of RCMs to successfully deliver a sustained release of growth/differentiation factor 5 with subsequent osteogenic effects on rat mandibular defects in vivo.[11] Our previous study demonstrated that RCMs containing stromal cell-derived factor-1 significantly facilitated bone regeneration in vivo, compared to that in the controls and RCM group.[12] Furthermore, the osteogenic effects of an RCM carrying a release factor, osteogenic protein-1, on rat mandibular bone defects in vivo have been reported. Thus, osteogenic protein-1-containing RCM may prove to be a useful device for bone regeneration with effective osteoinductive potency.[13]

A series of growth factors regulate bone development and regeneration in vivo.[14] Among the growth factors for tissue regeneration is fibroblast growth factor-2 (FGF-2), which induces neovascularization and osteogenesis.[15] FGF-2 can reportedly stimulate bone formation.[16] Moreover, some studies have demonstrated that FGF-2 significantly promotes new alveolar bone formation in chronic periodontitis patients in randomized clinical trials.[17] Several studies have also demonstrated that local application of recombinant FGF-2 incorporated into an appropriate carrier stimulates bone formation in a bone defect site.[18,19]

To further improve clinical outcomes and search for new candidate growth factors for an effective bone regeneration method, we developed a new regeneration device that combines an RCM containing FGF-2 (RCM/FGF-2) for bone regeneration. However, no data are available on the application of RCM/FGF-2 for critically-sized circular bone defects in vivo. Moreover, accurate real-time assessment of physical parameters, such as the volume of newly formed bone (NFB) and its mineral density at specified time intervals, provides extensive information about bone dynamics and the time required for osseous healing in bone defects.[20] However, there are no reported studies on real-time changes in NFB volumes and mineral densities using RCM/FGF-2 in standardized mandibular defect treatments in live animal models. Therefore, the aim of the present study was to investigate the ability of RCM/FGF-2 to promote bone regeneration in rat mandibular bone defects using real-time in vivo micro-computed tomography (micro-CT) and traditional histological evaluation.

Material and methods

Preparation of RCMs containing FGF-2

A commercially available RCM (BioMend®; Hakuho, Tokyo, Japan) consisting of cross-linked bovine type I collagen

was used for in vitro (size: 5 mm × 7.5 mm) and in vivo (size: 5 mm × 15 mm) studies. Low (0.5 μg, L) or high (2.0 μg, H) concentration of a carrier-free recombinant rat FGF-2 solution (R&D Systems, Minneapolis, MN, USA) was impregnated into the RCMs before beginning the experiment.

Release kinetics of FGF-2 from the RCMs using enzyme-linked immunosorbent assay (ELISA)

The in vitro release kinetics of FGF-2 from RCM was evaluated at 37 °C in 2 ml of phosphate buffered saline (PBS (pH 7.2); Fujifilm Wako Co., Osaka, Japan) for 2 weeks. At predetermined intervals, 2 ml PBS containing FGF-2 at 2, 4, 6, 10, and 14 days was withdrawn and renewed with an equal volume of fresh PBS. Samples were stored at −20 °C until testing. All collected samples were centrifuged and filtered to remove free-floating impurities, and analyzed quantitatively using a rat FGF-2 ELISA kit (R&D Systems, Minneapolis, MN, USA) at the end of the experiment. The data shown are the results of a single experiment (n = 3) that was conducted twice.

Study animals

A total of ten 10-week-old male Fischer 344jcl rats, each weighing of 250 ± 20 g, were used in this study. The animals were allowed to acclimatize to the laboratory environment for a period of 7 days at a temperature of 23—24 °C and humidity of 55% with 12 hourly dark—light cycles. The animals were housed in pairs, in a specific pathogen-free environment with access to standard commercial food and tap water *ad libitum*. The study protocol was approved by the local animal ethics committee under the Guidelines for Animal Experiments of Nihon University (AP14DEN035, AP17DEN030, AP19DEN13-2).

Surgical protocol

The rats were lightly anesthetized pre-operatively by inhaling isoflurane with O_2 and then deeply anesthetized by intraperitoneal (i.p.) application of a mixture of 0.15 mg/kg dexmedetomidine hydrochloride (Fujifilm Wako Co., Osaka, Japan), 2.0 mg/kg midazolam (Astellas Pharma Inc., Tokyo, Japan), and 2.5 mg/kg butorphanol tartrate (Meiji Seika

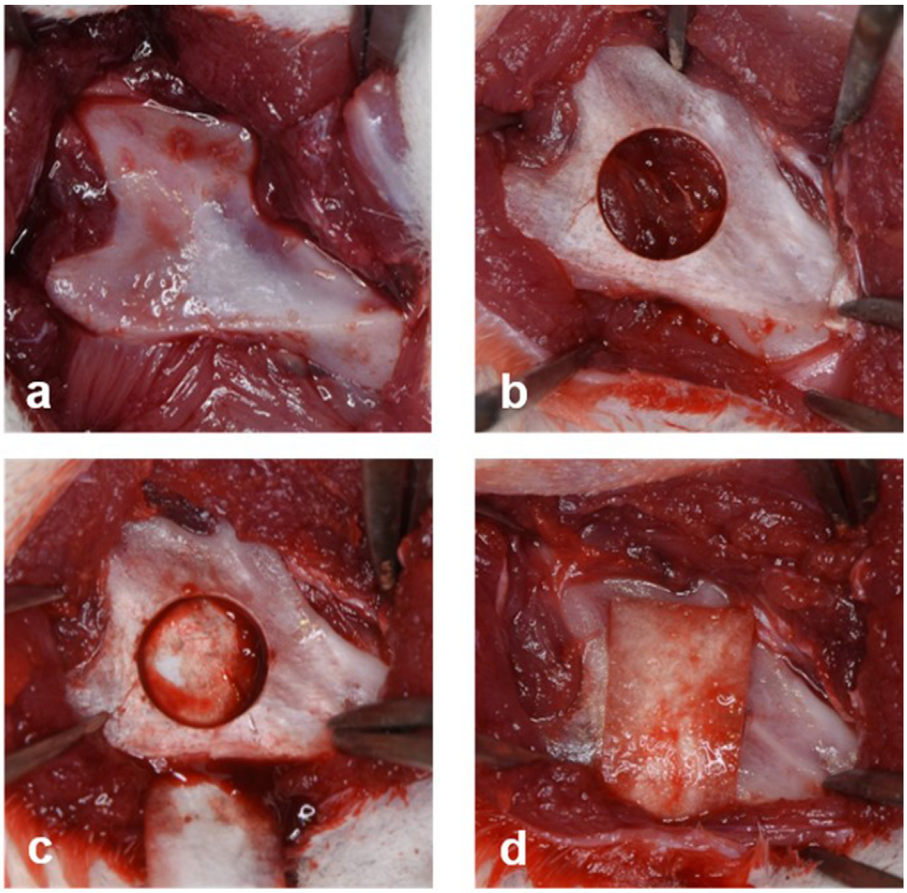

Figure 1 Surgical protocol. (a) After making an incision on the mandibular ramus, we created a full- thickness flap and reflection to expose the mandibular angle site. (b) An experimental defect of 4 mm diameter was created by using a trephine drill on the right side of the mandible ramus. (c) Placement of an inner resorbable collagen membrane between the mandibular bone and the underlying periosteum. (d) Placement of a resorbable collagen membrane completely over the circular bone defect at the mandibular angle.

Pharma Co., Tokyo, Japan). Anesthetic doses were strictly titrated based on the weight of the animal to eliminate adverse reactions resulting from general anesthesia. Intraperitoneal injection of 500 μl of a 1:80,000 dilution of lidocaine (Xylocaine; Astra Zeneca, Osaka, Japan) was administered to control bleeding and provide additional anesthesia. The surgical region was shaved and washed with 70% ethanol (Fujifilm Wako Co., Osaka, Japan) before surgical incision.

An incision was made in the skin using a sterile No. 15 surgical blade (Feather Co., Osaka, Japan). The incision included the entire thickness of the muscle around the mandibular angle and the underlying periosteum. We excised the skin and periosteum to expose the mandibular bone. After identifying of the anatomical landmarks, we created an experimental mandible bone defect on both sides using a 4.0 mm diameter bone trephine bur (Dentech, Tokyo, Japan) on a rotary handpiece under irrigation with 0.9% saline solution (Fujifilm Wako Co., Osaka, Japan).

In the membrane-treated groups, we covered the defect with a barrier membrane on the buccal and lingual sides (Fig. 1). After surgery, the muscle and skin layers were repositioned and closed using 5-0 resorbable sutures (Alfresa Pharma Co., Osaka, Japan). All animals were kept under observation until they recovered from anesthesia, after which they were returned to their cages. They were fed a commercial softened food diet for 7 days postoperatively, followed by a normal food diet until euthanization.

Their mandibular defects were randomly assigned to one of the following four experimental groups (5 rats per group): (1) control: no treatment, (2) RCM group: the defect was covered with RCM alone, (3) L-FGF-2 group: the defect was covered with RCM containing 0.5 μg FGF-2, and (4) H-FGF-2 group: the defect was covered with RCM containing 2.0 μg FGF-2.

Real-time in vivo micro-CT evaluation

The micro-CT scan sequence included a baseline scan, performed immediately after surgery, and follow-up scans, conducted at 2, 4, and 6 weeks postoperatively. Three-dimensional (3D) isosurface rendering and construction of images were performed using i-View software (Kitasenjyu Radist Dental Clinic; i-View Image Center, Tokyo, Japan), according to the manufacturer's recommendations. Representative sections were cut from the vertical view after 3D reconstruction. The standard resolution mode was used to quantify the microstructural properties of bone. The amount of new bone formation within the defect region was assessed using micro-CT (R_mCT2 system; Rigaku, Tokyo, Japan). The CT settings were as follows: pixel matrix, 480 × 480; voxel size, 30 × 30 × 30 μm; slice thickness, 120 μm; tube voltage, 90 kV; tube current, 100 μA; and exposure time, 17 s. The region of interest was chosen around the NFB, and the bone volume (BV) and bone mineral density (BMD) of the NFB within the circular defects from voxel images were automatically collected and measured using BV-measurement software (Kitasenjyu Radist Dental Clinic; i-View Image Center, Tokyo, Japan). NFB volumes (NBV) were measured in cubic millimeter (mm^3), and their BMD was measured in grams per cubic millimeter (mg/cm^3). Micro-CT imaging of the samples was regularly performed from baseline to 6 weeks after surgery.

Histological analysis

At the end of the observation period, 6 weeks after the defect operation, all animals were euthanized with carbon dioxide. The mandibular ramus was explanted and fixed in 10% neutral- buffered formalin solution (Fujifilm Wako Co., Osaka, Japan). After 14 days of fixation, histopathological examination was conducted on all mandibular defect sites. The samples were dissected and decalcified in K-CX (Falma, Tokyo, Japan) for 5 days. The decalcified samples were dehydrated with graded ethanol, defatted in xylene (Fujifilm Wako Co., Osaka, Japan), and embedded in paraffin. The embedded tissues were cut into 5-μm sections using a microtome. Serial sections were stained with hematoxylin and eosin for histological evaluation. Images were captured using a polarizing microscope (Eclipse LV100POL; Nikon

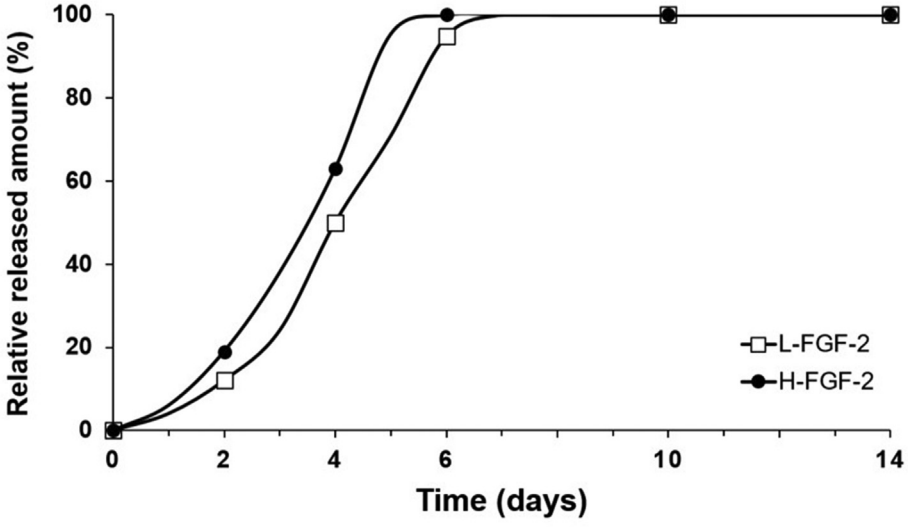

Figure 2 Recombinant rat FGF-2 release profile of the RCM containing FGF-2.

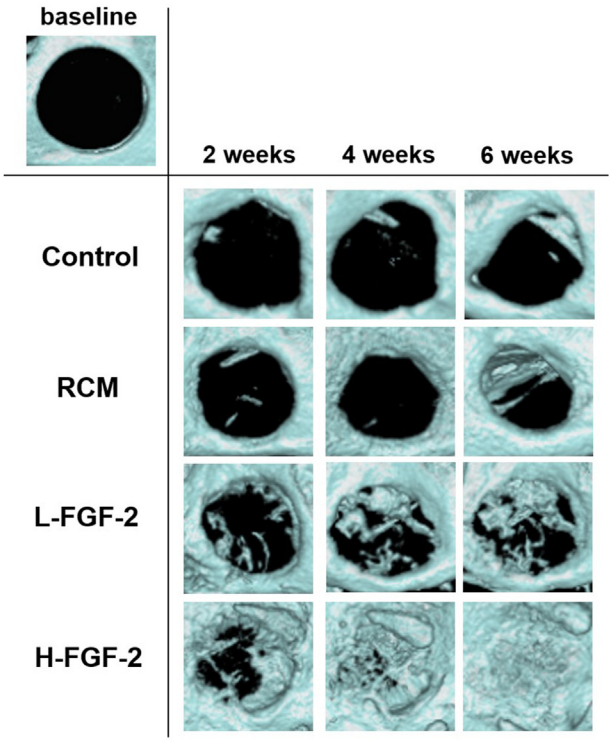

Figure 3 A series of reconstructed in vivo real-time micro-CT representative images of new bone formation in rat mandibular defects at baseline, 2, 4, and 6 weeks after surgical procedures in four groups: control, RCM alone, RCM containing a low dose of 0.5 μg of FGF-2 (L-FGF-2), and RCM containing a high dose of 2.0 μg of FGF-2 (H-FGF-2). The black color shows non-mineralized defects.

Instech Co., Ltd., Tokyo, Japan), and histology sections were analyzed at the Department of Pathology, Nihon University School of Dentistry.

Tartrate resistant acid phosphatase (TRAP) staining was performed using a commercial kit (Sigma-Aldrich, St. Louis, MO, USA). Positively-stained cells with three or more nuclei were identified as osteoclastic cells, and the number of osteoclasts was counted using ×40 magnification.

Histomorphometric analysis

NFB within the defects in each group was determined using micro-CT images and histological sections. In micro-CT analysis, new bone areas were measured by counting the number of pixels representing hard tissues within the NFB boundaries. In addition, the defect closure rate, determined by measuring the area within the circular bone defect edges, was designated as a percentage of the square of the gross defect. The new bone ratio in each of the measured areas described above was measured using ImageJ software (National Institutes of Health, Bethesda, MD, USA).

Immunohistochemical procedures

Immunohistochemical procedures were performed on histological sections exhibiting bone formation. Longitudinal sections of the paraffin-embedded mandible (5 μm) were incubated at 60 °C for 24 h. This was followed by defatting in xylene and hydration with graded ethanol (100%—70%). Following deparaffinization with xylene, the sections were rehydrated using a graded series of ethanol and washed in distilled water. Endogenous peroxidase (Fujifilm Wako Co., Osaka, Japan) was blocked by incubating the sections with 0.3% H_2O_2. After washing the sections with PBS, they were treated with normal horse serum for 30 min to prevent non-specific binding. Primary antibodies (mouse monoclonal antibodies against osteocalcin (OCN); Takara Bio Inc., Shiga, Japan) were diluted 1:100 in PBS containing 1.0% bovine serum albumin (Fujifilm Wako Co., Osaka, Japan) and incubated overnight at room temperature. Each section was then rinsed thrice with PBS for 3 min, incubated with biotinylated anti-rat immunoglobulin (IgG; Abcam, Tokyo, Japan) for 30 min in a moist chamber, and incubated with horseradish peroxidase streptavidin conjugate for 30 min. The slides were then rinsed with PBS. The antibody complexes were visualized using 3,3′-diaminobenzidine substrate and $H_2O_{2.,}$ washed in distilled water, and counterstained with hematoxylin (Fujifilm Wako Co., Osaka, Japan). For controls, the sections were treated using the aforementioned protocol without incubation with primary antibodies. The stained sections were analyzed using optical microscopy and photographed.

Statistical analysis

Each value represents the mean ± standard error (S.E.M). NBV, BMD, and the defect closure rate among the groups were compared using a two-way analysis of variance (ANOVA) to identify differences in the parameters within each study group and between groups. A significance level of 0.05 was used for all statistical comparisons. Post-hoc analysis using the Tukey's method was performed to detect pairs of groups with a statistical difference. All statistical analyses were performed with GraphPad Prism 5 software (GraphPad Inc., La Jolla, CA, USA). For all statistical analyses, p values less than 0.05 were considered significant.

Results

In vitro release profile of FGF-2 from RCMs

Fig. 2 shows the kinetic release of FGF-2 in vitro. RCM containing FGF-2 exhibited a sustained release profile for the two different effective doses (0.5 or 2.0 μg) during the 1- to 14-day period. The cumulative release of FGF-2 from RCM reached approximately 100% within 6 days, followed by a gradual decrease.

In vivo effect of RCM/FGF-2 on bone regeneration

Representative images from the micro-CT scan of the mandibular defects in rats from baseline to 6 weeks are shown in Fig. 3. Based on the structural morphology of the defects, we inferred that the isolated islands of particulates in the defects were NFB. Examination of the RCM/FGF-2 groups indicated that bone formation in the FGF-2-

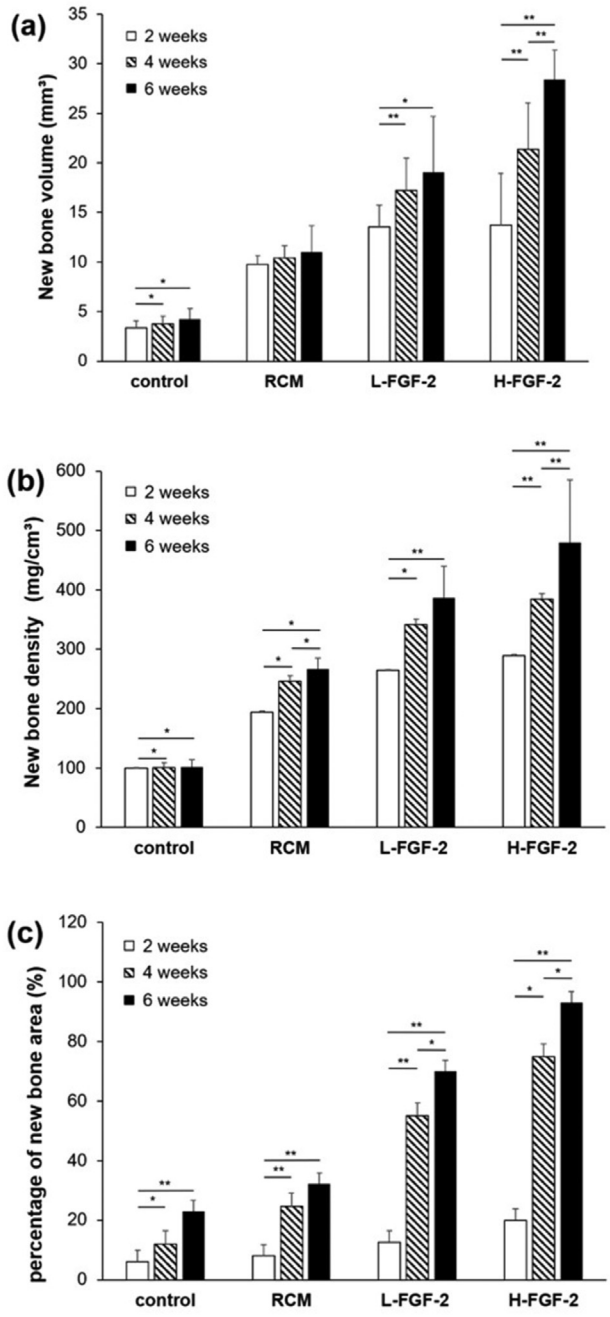

Figure 4 The quantitative micro-CT analysis of new bone formation, (a) bone volume (mm^3), (b) new bone density (mg/cm^3), and (c) the percentage of new bone area (%) in rat mandible defects treated with RCM/FGF-2 throughout the experimental period. Four groups were compared: Control, RCM alone, RCM containing 0.5 μg FGF-2 (L-FGF-2), and RCM containing 2.0 μg FGF-2 (H-FGF-2). $^*p < 0.05$ and $^{**}p < 0.01$.

treated defects was higher than that in the control or RCM groups. However, the NFB in the H-FGF-2 group was higher than that in the L-FGF-2 group. Moreover, new bone filled the defects at 6 weeks after surgery in the H-FGF-2 group. These observations are consistent with the quantitative results shown in Fig. 4.

The micro-CT analysis results revealed an increase in NBV within the mandibular defects throughout the study period in all groups (Fig. 4 and Table 1). At 6 weeks, the highest NBV was observed in the H-FGF-2 group ($28.39 \pm 2.97\ mm^3$), followed by the L-FGF-2 ($19.05 \pm 5.65\ mm^3$), RCM alone ($11.00 \pm 2.65\ mm^3$), and control groups ($4.22 \pm 1.06\ mm^3$). The NBV in the FGF-2-treated groups was significantly higher than that in the control group throughout the study, with higher bone formation in the H-FGF-2 group than that in the L-FGF-2 group. In addition, there was a significant increase in the NBV from baseline at 6 weeks in the H-FGF-2 groups ($p < 0.01$), and as early as 2 weeks in the RCM and L-FGF-2 groups ($p < 0.05$). During weeks 2 and 4, the NBVs in the FGF-2-treated groups were significantly higher than those in the control and RCM groups ($p < 0.05$). The highest increase in NBV occurred within the first 2 weeks in all the test groups. Table 2 illustrates the rate of increase in NBVs. The BMD of the NFB increased from baseline to 6 weeks in both the control and test groups (Fig. 4 and Table 1). At 6 weeks, the H-FGF-2 group had the highest BMD ($480.30 \pm 49.48\ mg/cm^3$), followed by L-FGF-2 ($386.16 \pm 105.03\ mg/cm^3$), RCM ($266.80 \pm 9.32\ mg/cm^3$), and control groups ($101.37 \pm 1.64\ mg/cm^3$). We observed significant increases in BMD of NFB compared with baseline by week 2 in all groups, except for the control group. Similar to NBV, the highest increase in BMD of NFB among the groups occurred within the first 2 weeks after surgery (Table 2). The H-FGF-2 group increased rapidly between weeks 4 and 6, leading to statistically significant differences compared to the baseline values ($p < 0.01$). At 6 weeks, the new bone area fraction for the RCM/FGF-2 groups significantly increased compared to the control and RCM groups ($p < 0.05$, and $p < 0.01$, respectively). Moreover, the H-FGF-2 group had the highest amount of new bone area fraction ($93.03\% \pm 4.76\%$), which was approximately 4-fold higher than that in the RCM group ($20.93\% \pm 3.82\%$) ($p < 0.01$). Moreover, the RCM/FGF-2 groups had significantly higher new bone area fractions than that the control group ($p < 0.01$). Furthermore, the ratio in the H-FGF-2 group was markedly higher than that in the L-FGF-2 group at 4 and 6 weeks ($p < 0.05$; Fig. 4 and Table 1).

Histological findings

Histological evaluations of the experimental groups were performed to assess the osteogenic status of the regenerated tissue within the defect sites. No adverse tissue reactions were observed. In the RCM/FGF-2 groups, mature new bone was integrated with the host bone at the marginal aspect of the defect. Notably, in the images of H-FGF-2, mature new bone developed, and bone marrow cavity-like morphology was observed in the marginal aspect of the defects. The mature new bone was significantly higher in the RCM/FGF-2 groups than in the RCM and control groups. Furthermore, in the FGF-2 treated groups, osteoblasts, osteocytes and blood vessels were found within the NFB (Fig. 5).

The representative TRAP staining images at 6 weeks post-surgery are shown in Fig. 6. The red stains indicate positive staining of osteoclasts. In the control group, large populations of TRAP- positive osteoclasts were located

Table 1 Volume, mineral density, and percentage of area parameters for newly formed bone in four groups at different data collection periods.

Test groups (n = 5 per group)	Data collection period (weeks)	Newly formed bone [mean (SD)]		
		Volume (mm^3)	Mineral density (mg/mm^3)	Area (%)
Control	0	—	—	—
	2	3.34 (0.73)	99.31 (1.20)	6.28 (2.13)
	4	3.77 (0.72)[c]	100.32 (1.28)[c]	12.00 (2.44)[c]
	6	4.22 (1.06)	101.37 (1.64)[c]	23.63 (2.95)[a,d]
RCM	0	—	—	—
	2	9.74 (0.92)[a]	194.31 (9.10)[a]	8.21 (2.87)[a]
	4	10.38 (1.25)[a]	245.86 (9.87)[a,c]	24.70 (3.99)[a,d]
	6	11.00 (2.65)[a]	266.80 (9.32)[a,c,e]	32.25 (4.99)[a,d]
L-FGF-2	0	—	—	—
	2	13.56 (2.13)[a]	264.73 (18.55)[a]	12.60 (2.82)[a]
	4	17.19 (3.29)[a,d]	341.16 (53.71)[a,c]	55.24 (3.49)[b,d,e]
	6	19.05 (5.65)[a,c]	386.16 (105.03)[a,d]	70.51 (3.65)[b,d]
H-FGF-2	0	—	—	—
	2	13.73 (5.20)[a]	289.67 (70.38)[a]	20.93 (3.82)[a]
	4	21.38 (4.67)[a,d]	384.84 (40.16)[b,d]	74.80 (4.39)[b,c,e]
	6	28.39 (2.97)[b,d,f]	480.13 (49.48)[b,d,f]	93.03 (4.76)[b,d]

RCM = Resorbable collagen membrane; L-FGF-2 = RCM containing 0.5 μg of fibroblast growth factor-2 (FGF-2); H-FGF-2 = RCM containing 2.0 μg of FGF-2; SD= Standard deviation.

[a] Statistically significant increase compared with baseline ($p < 0.05$).
[b] Statistically significant increase compared with baseline ($p < 0.01$).
[c] Statistically significant increase compared with 2 weeks ($p < 0.05$).
[d] Statistically significant increase compared with 2 weeks ($p < 0.01$).
[e] Statistically significant increase compared with 4 weeks ($p < 0.05$).
[f] Statistically significant increase compared with 4 weeks ($p < 0.01$).

adjacent to the edge of the defects. However, FGF-2 treated groups showed significantly fewer osteoclasts than those in the control and RCM groups ($p < 0.01$; Fig. 6b).

Positive immunoreactivity for osteocalcin, a marker for mature bone formation, was evident in the FGF-2 treated groups at 6 weeks after surgery (Fig. 7). Intense OCN staining was observed near the NFB in the group with FGF-2 delivery.

Discussion

The present study hypothesized that RCM/FGF-2 promotes osseous regeneration in standardized rat mandibular defects. To the best of our knowledge, the present study is the first to perform a real-time in vivo micro-CT experiment to elucidate the efficacy of RCM/FGF-2, RCM alone, and control in GBR around mandibular osseous defects at 6 weeks after surgery. Furthermore, the mandible is a unique bone that carries a significant masticatory load. Therefore, the data obtained for other bones (e.g., calvarial defects) may not apply to the mandible.[21] Micro-CT analysis revealed homogeneously distributed new bone formation within the standardized mandibular defects as early as 2 weeks in the RCM/FGF-2 groups, while it was observed only at the peripheries of the circular bone defects in the control and RCM groups. Moreover, our study revealed progressively increasing amounts of new bone formation, BMD, and percentage of new bone area within the standardized mandibular defects in the RCM/FGF-2 groups. These enhancements in bone regeneration occurred in the FGF-2-treated groups with increasing FGF-2 concentrations. The real-time micro-CT images revealed radiopacities in the L-FGF-2 group with less bone formation inside the defects than those in the H-FGF-2 group. Similar volumes of new bone formation were observed between the two groups at 2 weeks, followed by a rapid increase until 6 weeks in the H-FGF-2 group. Moreover, there were similarities BMD of the L-FGF-2 and H-FGF-2 groups. Furthermore, the RCM/FGF-2-treated groups had significantly increased bone regeneration within the mandibular defects than that in the control and RCM groups. These findings indicate that RCM/FGF-2 enhances new bone formation in rat mandibular defects in the early postoperative phase.

The main biological function of GBR membranes is to provide a physical barrier against the surrounding environment, which both prevents the ingrowth of soft tissue and loss of inherent healing factors, consequently promoting bone tissue ingrowth.[22] In circular mandibular defects with a barrier membrane, osteoprogenitor cells originating from the adjacent bone play an important role in populating and regenerating these defects with NFB. However, the new bones failed to fill the untreated defects throughout the experimental period and were prone to fibrous tissue invasion. The micro-CT results obtained from the control group corroborated the above findings. Histological observations indicated that only a slight amount of fibrous connective tissue invaded the defects in the RCM/FGF-2-treated groups.

Table 2 Mean rates of change in volume, mineral density, and the percentage of area parameters for newly formed bone in four groups at different data collection periods.

Test groups (n = 5 per group)	Data collection period (weeks)	Newly formed bone [mean (SD)]		
		Rate of increase in volume (mm^3/week)	Rate of increase in mineral density (mg/mm^3/week)	Percentage of area (%/week)
Control	0–2	3.34	99.31	6.28
	2–4	0.43	1.01	5.72
	4–6	0.45	1.05	11.63
RCM	0–2	9.74	194.31	8.21
	2–4	0.64	51.55	16.49
	4–6	0.62	20.94	7.55
L-FGF-2	0–2	13.56	264.73	12.60
	2–4	3.63	76.43	42.64
	4–6	1.86	45.00	15.27
H-FGF-2	0–2	13.73	289.67	20.93
	2–4	7.65	95.17	53.87
	4–6	7.01	95.29	18.23

RCM = Resorbable collagen membrane; L-FGF-2 = RCM containing 0.5 μg of fibroblast growth factor-2 (FGF-2); H-FGF-2 = RCM containing 2.0 μg of FGF-2.

Conversely, there were notable levels of soft tissues, muscles, and connective tissues in the defects of the control group. The untreated defects proved the critical nature of the defect model used in this study, as the control group defects failed to heal completely, even at the study endpoint (6 weeks). Some studies have claimed that the defect ≧4 mm in diameter in the mandibular sites is a critical size for evaluating bone healing in the GBR treatment model.[23,24] Kellomäki et al.,[25] reported directional bone growth by osteoblasts in close contact with adjacent bone using a bioabsorbable membrane inserted in a bone defect, suggesting that osteoblasts convert to bone tissues following membrane degradation. In the present study, histological sections of the defect covered with RCM revealed that the defect was mostly filled with cells, extracellular matrix components, fibrous connective tissues, and mineralized new bone. This resorbable membrane can effectively direct and populate cells around the defect sites and trigger the secretion of an appropriate tissue matrix, leading to the recovery of the function of damaged tissues, and osteoblasts accumulating around the RCM. Therefore, we observed mature bone formation throughout the experimental period.

FGF-2, also known as basic FGF (bFGF), is the most common FGF ligand used in regenerative medicine, including bone regeneration. FGF-2 does not exhibit an osteoinductive properties, and functions as an accelerator of osteogenesis under appropriate conditions. Previous studies have shown that FGF-2 is an endogenous, positive regulator of bone mass that promotes the proliferation of osteoblast cell lineage and induction of angiogenesis.[26,27] FGF-2-knockout mice exhibited a significant decrease in bone mass and bone formation. Bone marrow stromal cells from these mice demonstrated decreased osteoblast differentiation, which can be partially recovered by adding exogenous FGF-2 in vitro.[28] Certain in vivo experiments demonstrate the application of FGF-2 for the treatment of non-critical- and critical-sized bone defects. Murahashi et al. recently showed that multi-layered poly (L-lactic acid) nanosheets loaded with recombinant human FGF-2 (rhFGF-2) effectively enhanced bone regeneration in mouse femoral bone defects.[29] Other experiments demonstrated that co-poly lactic acid/glycolic acid-coated scaffolds loaded with FGF-2 exhibited significant bone augmentation in a rat calvaria defect model and an FGF-2-loaded scaffold stimulated woven trabecular bone formation in histological observation.[30] Kawaguchi et al.[31] reported the first prospective multicenter clinical trial on the effect of rhFGF-2 in promoting bone formation for knee osteoarthritis. In the field of dentistry, rhFGF-2 has a strong regenerative action in alveolar bones with no notable safety issues.[17] Further, the results from our study corroborate with the bone regeneration properties of FGF-2 reported in several animal[29,30] and clinical studies.[17,31] Therefore, FGF-2 acts in concert with RCMs in rat mandibular bone defects for bone regeneration.

The use of several collagen-based carriers with FGF-2 for GBR has been debated in the literature. According to Kobayashi,[32] an FGF-2-loaded collagen gel-sponge composite scaffold stimulates bone augmentation in a cranial bone defect. Moreover, histological findings in this study revealed that an FGF-2-loaded collagen scaffold promptly enhanced osteoblastic and fibroblastic cell proliferation into the collagen scaffold. A recent study reveals that collagen-binding bFGF with composite material effectively promotes bone regeneration of horizontal bone defects in rats, possibly through the sustained release of bFGF.[33] Collectively, collagen-based biomaterials are considered a useful delivery vehicle for growth factors, including FGF-2. In the present experimental results, we presumed that RCM/FGF-2 is responsible for maintain the sustained release of FGF-2 within a mandibular defect area for a fixed period. Based on the results of defect closure and bone formation, which were enhanced significantly by FGF-2 within the membrane, we infer that FGF-2 is effective for the bone regeneration process. In

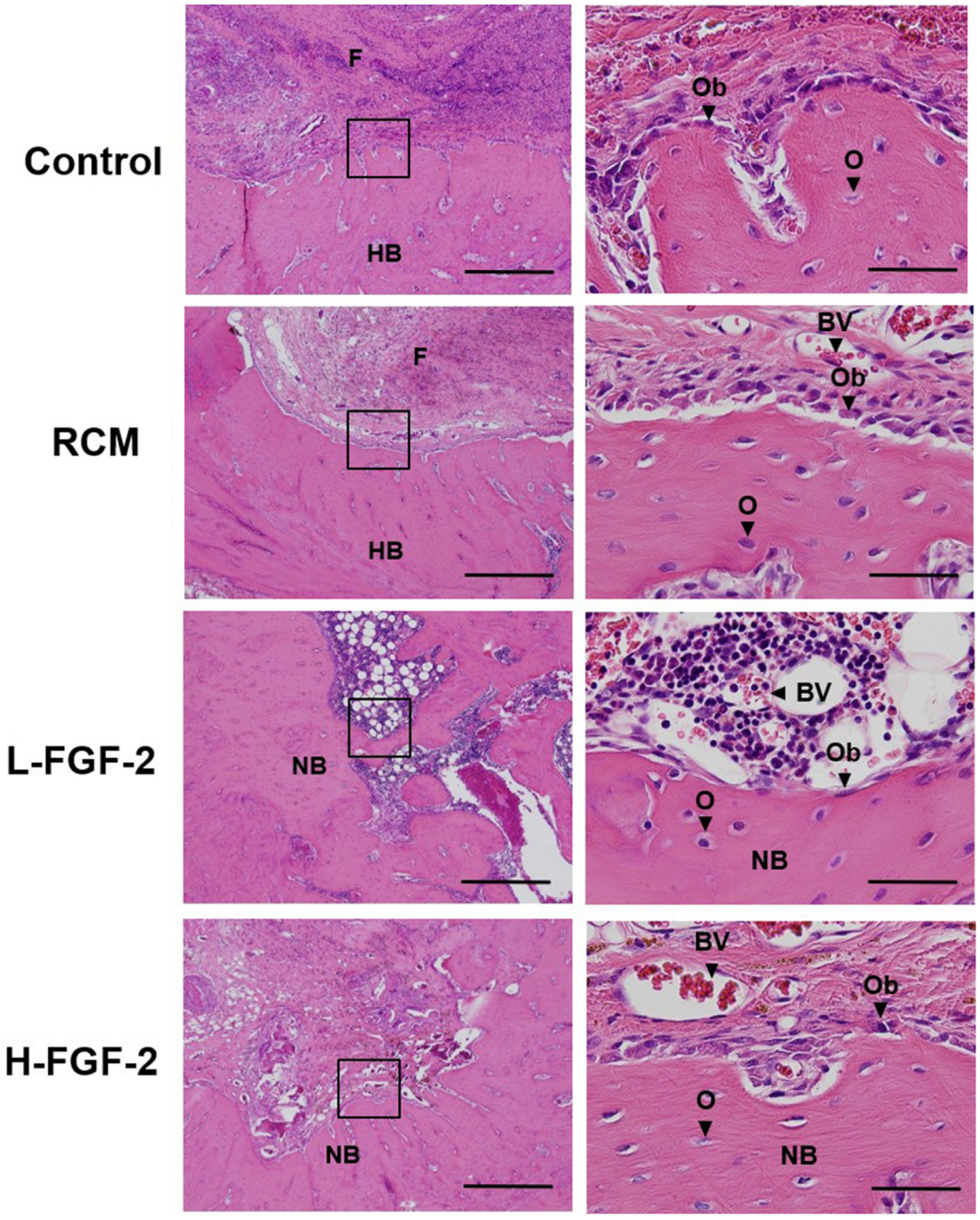

Figure 5 Light microscopic images (×4—40) show regenerated bone at 6 weeks after applying of RCM/FGF-2 at rat mandibular bone defects. NFB at the periphery of a mandibular defect was observed in FGF-2 treated groups. In addition, in the H-OP-1 group, mature lamella bone was seen and the defect tended to coalesce with the NFB. L-OP-1 showed similar effects with the newly formed mature bone. The specimens were stained with hematoxylin and eosin (HE). Scale burs indicate 100 μm and 50 μm in low- and high-magnification images, respectively. HB: host bone, NB: Newly formed bone, F: fibrous tissue, Ob: Osteoblast, O: Osteocyte, BV: Blood vessel. Representative histological sections of RCM/FGF-2 treatment groups at high magnification (40×) showing NB, Ob, O, and BV.

addition to the bioactive role of the RCM/FGF-2 composite, this study suggests that FGF-2 play a stimulatory role in bone regeneration. Although more systematic research on the in vitro and in vivo release profile of FGF-2 and its dose-dependent effects are required, the results of our study demonstrated the potential of RCM/FGF-2 as a novel GBR membrane.

The qualitative findings of in vivo micro-CT were further confirmed by histological findings, which showed abundant amounts of NFB, osteoblasts, osteoclasts, osteocytes and blood vessels in the matrix, covering the areas of the mandibular defect in the RCM/FGF-2 groups. Previous reports have shown that FGF-2 can regulate osteoblast differentiation and osteocyte formation.[34] Furthermore, we

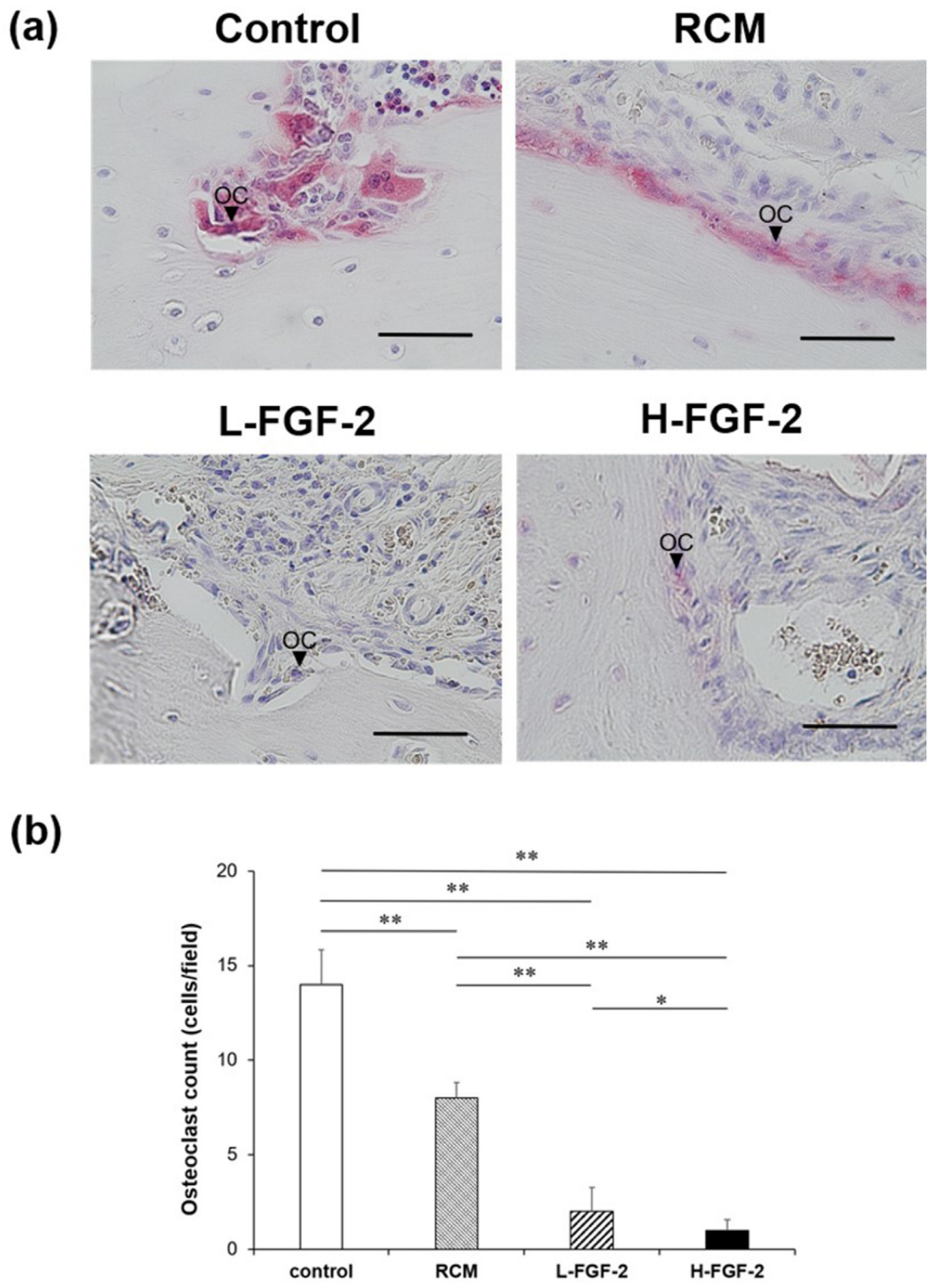

Figure 6 The TRAP staining at 6 weeks (a) and osteoclast density (b). The red staining indicated positive TRAP staining of osteoclasts in the defect area. The RCM/FGF-2 group exhibited the highest amount of new bone at 6 weeks but exhibited the lowest number of osteoclasts. The control group had the lowest amount of new bone and the highest number of osteoclasts. Each value is the mean $\pm$ SD (n $=$ 5). Scale bars indicate 50 μm in the figures.

detected many blood vessels in NFB in the RCM-FGF-2-treated groups after 6 weeks. The generation of blood vessels is essential for bone repair and osteogenesis during normal bone development.[35] Further, FGF-2 showed positive effects on bone repair and angiogenesis in a dose- and time-dependent manner and with the use of different species, carriers, and model systems.[36,37] Therefore, it is possible that NFB in the FGF-2-treated defect might be associated with the level of vascularization by FGF-2.

TRAP, a glycosylated metalloenzyme, is highly expressed in osteoclasts and widely used as a specific marker of osteoclasts in bone.[38] Consistent with certain previous studies,[39,40] our study revealed that FGF-2 inhibits TRAP-positive osteoclasts during osteoclastogenesis.

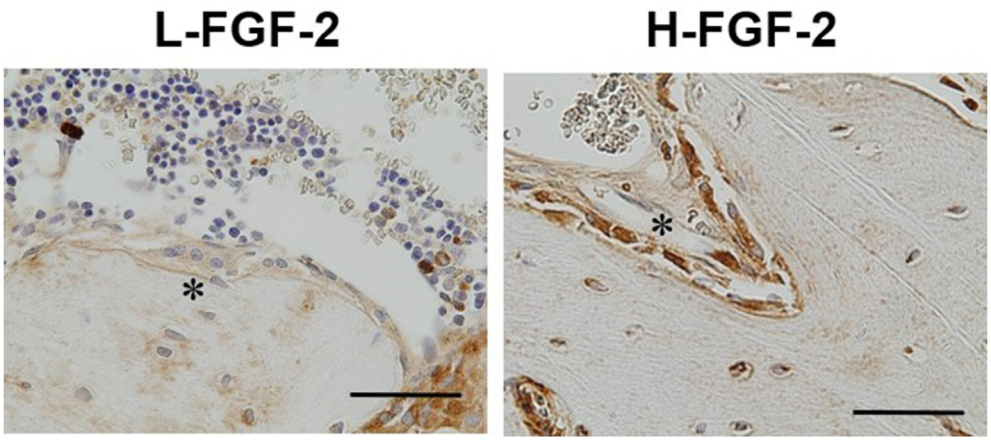

Figure 7 Effect of FGF-2 on bone maturation and mineralization. The immunohistochemistry results for osteocalcin (OCN) at 6 weeks. OCN immunoreactivity was obvious in the FGF-2 treated groups (asterisk). Scale bars indicate 50 μm in figures.

OCN is the main protein of the collagen matrix derived from cell growth and is a specific marker of bone formation and resorption. An increase in its level accelerates osteoblastic activity and bone remodeling.[41] The effects of RCM/FGF-2 on OCN expression suggested the continuous process of FGF-2 induced bone formation and maturation during the experimental period. In our study, stronger immunostaining of OCN was detected at 6 weeks in the RCM/FGF-2 groups, suggesting improved bone regeneration. Non-collagenous proteins play an important role in the remodeling process of NFB at the mandibular bone defect sites. FGF-2 significantly increased OCN gene expression of human periodontal ligament cells in vitro.[42] Moreover, Cantatore et al.[43] reported that OCN levels increased after fracture and remained high during the bone healing period. Thus, angiogenic activity might have a crucial role in bone regeneration. We speculate that the bone regeneration of this mandibular osseous defect may be influenced by the interaction between OCN and FGF-2-induced angiogenesis.

This study had several limitations. The main findings cannot be directly transferred to humans, as there are significant differences in the functional anatomy and increased bone turnover in rats compared to those in humans. The number of samples included in the final analysis was relatively small with marked individual variability for some parameters. The number of animals should be reduced to the minimum required to achieve a statistically significant result. When conducting animal studies, the principles of the three Rs (Reduction, Replacement and Refinement) must be applied.[44] All rats were sacrificed before histological examination, therefore, there was no possibility for a longitudinal study of the bone microstructural changes in each animal during the observation periods.

The present study reveals significantly enhanced qualitative and quantitative bone regeneration in the standardized rat mandibular bone defect using a novel regeneration unit of RCM/FGF-2. The addition of an FGF-2 component significantly enhanced bone formation at 6 weeks after application. Furthermore, incorporation of FGF-2 at an appropriate concentration within the RCMs enhanced bone regeneration and complete closure of defects. These findings affirmed the value of this study for its clinical applications ranging from the regeneration of osseous defects to ridge augmentation and dental implant with sufficient quantities of alveolar bone.

Declaration of competing interest

The authors have no conflicts of interest relevant to this article.

Acknowledgments

We thank the Department of Oral Health Sciences, Nihon University School of Dentistry, for technical advice and assistance, and the Department of Pathology, Nihon University School of Dentistry, for histological imaging. We also thank Prof. Yoshinori Arai who assisted and commented on the micro-CT analysis. We thank the Ito Bone Histomorphometry Institute for analyzing histological sections of newly formed bone.

This research was supported in part by a Grant-in-Aid for Scientific Research (C) (No. JP19K10134 to T. Takayama) from the Ministry of Education, Culture, Sports, Science, and Technology (MEXT) of Japan, Grant from Dental Research Center, Nihon University School of Dentistry (to T. Takayama), and the Sato Fund, Nihon University School of Dentistry (to T. Takayama).

References

1. Chiapasco M, Zaniboni M, Boisco M. Augmentation procedures for the rehabilitation of deficient edentulous ridges with oral implants. *Clin Oral Implants Res* 2006;17:136—59.
2. Hämmerle CH, Jung RE. Bone augmentation by means of barrier membranes. *Periodontol* 2000;33:36—53. 2003.
3. Liu J, Kerns DG. Mechanisms of guided bone regeneration:a review. *Open Dent J* 2014;8:56—65.
4. Wang HL, Carroll MJ. Guided bone regeneration using bone grafts and collagen membranes. *Quintessence Int* 2001;32:504—15.
5. Saulacic N, Fujioka-Kobayashi M, Kobayashi E, Schaller B, Miron RJ. Guided bone regeneration with recombinant human

bone morphogenetic protein 9 loaded on either deproteinized bovine bone mineral or a collagen barrier membrane. *Clin Implant Dent Relat Res* 2017;19:600—7.
6. Urban IA, Monje A. Guided bone regeneration in alveolar bone reconstruction. *Oral Maxillofac Surg Clin* 2019;31:331—8.
7. Wessing B, Lettner S, Zechner W. Guided bone regeneration with collagen membranes and particulate graft materials: a systematic review and meta-analysis. *Int J Oral Maxillofac Implants* 2018;33:87—100.
8. Urban IA, Wessing B, Alandez N, et al. A multicenter randomized controlled trial using a novel collagen membrane for guided bone regeneration at dehisced single implant sites: outcome at prosthetic delivery and at 1-year follow-up. *Clin Oral Implants Res* 2019;30:487—97.
9. Khorsand B, Elangovan S, Hong L, Kormann M, Salem AK. A bioactive collagen membrane that enhances bone regeneration. *J Biomed Mater Res B Appl Biomater* 2019;107:1824—32.
10. Takata T, Wang HL, Miyauchi M. Migration of osteoblastic cells on various guided bone regeneration membranes. *Clin Oral Implants Res* 2001;12:332—8.
11. Yamano S, Haku K, Yamanaka T, et al. The effect of a bioactive collagen membrane releasing PDGF or GDF-5 on bone regeneration. *Biomaterials* 2014;35:2446—53.
12. Takayama T, Dai J, Tachi K, et al. The potential of stromal cell-derived factor-1 delivery using a collagen membrane for bone regeneration. *J Biomater Appl* 2017;31:1049—61.
13. Ozaki M, Takayama T, Yamamoto T, et al. A collagen membrane containing osteogenic protein-1 facilitates bone regeneration in a rat mandibular bone defect. *Arch Oral Biol* 2017;84:19—28.
14. Khojasteh A, Behnia H, Naghdi N, Esmaeelinejad M, Alikhassy Z, Stevens M. Effects of different growth factors and carriers on bone regeneration:a systematic review. *Oral Surg Oral Med Oral Pathol Oral Radiol* 2013;116:e405—23.
15. Gospodarowicz D, Neufeld G, Schweigerer L. Fibroblast growth factor: structural and biological properties. *J Cell Physiol* 1987;5:15—26.
16. Canalis E, Centrella M, McCarthy T. Effects of basic fibroblast growth factor on bone formation in vitro. *J Clin Invest* 1988;81:1572—7.
17. Kitamura M, Akamatsu M, Machigashira M, et al. FGF-2 stimulates periodontal regeneration: results of a multi-center randomized clinical trial. *J Dent Res* 2011;90:35—40.
18. Kinoshita Y, Matsuo M, Todoki K, et al. Alveolar bone regeneration using absorbable poly (L-lactide-co-ε-caprolactone)/β-tricalcium phosphate membrane and gelatin sponge incorporating basic fibroblast growth factor. *Int J Oral Maxillofac Surg* 2008;37:275—81.
19. Hosokawa R, Kikuzaki R, Kimoto T, et al. Controlled local application of basic fibroblast growth factor (FGF-2) accelerates the healing of GBR. *Clin Oral Implants Res* 2000;11:345—53.
20. Ru N, Liu SSY, Zhuang L, Li S, Bai Y. In vivo microcomputed tomography evaluation of rat alveolar bone and root resorption during orthodontic tooth movement. *Angle Orthod* 2013;83:402—9.
21. Kaban LB, Glowacki J. Induced osteogenesis in the repair of experimental mandibular defects in rats. *J Dent Res* 1981;60:1356—64.
22. Retzepi M, Donos N. Guided bone regeneration: biological principle and therapeutic applications. *Clin Oral Implants Res* 2010;21:567—76.
23. Kustro T, Kiss T, Chernohorskyi D, Chepurnyi Y, Helyes Z, Kopchak A. Quantification of the mandibular defect healing by micro-CT morphometric analysis in rats. *J Cranio-Maxillo-Fac Surg* 2018;46:2203—13.
24. Zhang W, Zhang Z, Chen S, Macri L, Kohn J, Yelick PC. Mandibular jaw bone regeneration using human dental cell-seeded tyrosine-derived polycarbonate scaffolds. *Tissue Eng Part A* 2016;22:985—93.
25. Kellomäki M, Niiranen H, Puumanen K, Ashammakhi N, Waris T, Törmälä P. Bioabsorbable scaffolds for guided bone regeneration and generation. *Biomaterials* 2000;21:2495—505.
26. Ornitz DM, Marie PJ. Fibroblast growth factor signaling in skeletal development and disease. *Genes Dev* 2015;29:1463—86.
27. Fei Y, Xiao L, Doetschman T, Coffin DJ, Hurley M. Fibroblast growth factor 2 stimulation of osteoblast differentiation and bone formation is mediated by modulation of the Wnt signaling pathway. *J Biol Chem* 2011;286:40575—83.
28. Montero A, Okada Y, Tomita M, et al. Disruption of the fibroblast growth factor-2 gene results in decreased bone mass and bone formation. *J Clin Invest* 2000;105:1085—93.
29. Murahashi Y, Yano F, Nakamoto H, et al. Multi-layered PLLA-nanosheets loaded with FGF-2 induce robust bone regeneration with controlled release in critical-sized mouse femoral defects. *Acta Biomater* 2019;85:172—9.
30. Yoshida T, Miyaji H, Otani K, et al. Bone augmentation using a highly porous PLGA/β-TCP scaffold containing fibroblast growth factor-2. *J Periodontal Res* 2015;50:265—73.
31. Kawaguchi H, Jingushi S, Izumi T, et al. Local application of recombinant human fibroblast growth factor-2 on bone repair: a dose-escalation prospective trial on patients with osteotomy. *J Orthop Res* 2007;25:480—7.
32. Kobayashi N, Miyaji H, Sugaya T, Kawanami M. Bone augmentation by implantation of an FGF2-loaded collagen gel-sponge composite scaffold. *J Oral Tissue Eng* 2010;8:91—101.
33. Nakamura S, Ito T, Okamoto K, et al. Acceleration of bone regeneration of horizontal bone defect in rats using collagen-binding basic fibroblast growth factor combined with collagen scaffolds. *J Periodontol* 2019;90:1043—52.
34. Ikpegbu E, Basta L, Clements DN, et al. FGF-2 promotes osteocyte differentiation through increased E11/podoplanin expression. *J Cell Physiol* 2018;233:5334—47.
35. Hankenson KD, Dishowitz M, Gray C, Schenker M. Angiogenesis in bone regeneration. *Injury* 2011;42:556—61.
36. Norrby K. Basic fibroblast growth factor and de novo mammalian angiogenesis. *Microvasc Res* 1994;48:96—113.
37. Inui K, Maeda M, Sano A, et al. Local application of basic fibroblast growth factor minipellet induces the healing of segmental bony defects in rabbits. *Calcif Tissue Int* 1998;63:490—5.
38. Minkin C. Bone acid phosphatase:tartrate-resistant acid phosphatase as a marker of osteoclast function. *Calcif Tissue Int* 1982;34:285—90.
39. Zuo J, Jiang J, Dolce C, Holliday S. Effects of basic fibroblast growth factor on osteoclasts and osteoclast-like cells. *Biochem Biophys Res Commun* 2004;318:162—7.
40. Nakagawa N, Yasuda H, Yano K, et al. Basic fibroblast growth factor inhibits osteoclast formation induced by 1alpha,25-dihydroxyvitamin D3 through suppressing the production of osteoclast differentiation factor. *Biochem Biophys Res Commun* 1999;265:45—50.
41. Brennan-Speranza TC, Conigrave AD. Osteocalcin: an osteoblast-derived polypeptide hormone that modulates whole body energy metabolism. *Calcif Tissue Int* 2015;96:1—10.
42. An S, Huang X, Gao Y, Ling J, Huang Y, Xiao Y. FGF-2 induces the proliferation of human periodontal ligament cells and modulates their osteoblastic phenotype by affecting Runx2 expression in the presence and absence of osteogenic inducers. *Int J Mol Med* 2015;36:705—11.
43. Cantatore FP, Crivellato E, Nico B, Ribatti D. Osteocalcin is angiogenic in vivo. *Cell Biol Int* 2005;29:583—5.
44. Rowan AN. The concept of the three R's. An introduction. *Dev Biol Stand* 1980;45:175—80.